Chapter 7
Microclimatology

Microclimatology investigates mean states and permanent repeated phenomena on the micrometeorological scale. These are small-scale circulation systems such as mountain and valley winds, land-sea wind circulations, and katabatic winds. These phenomena are the subjects of many textbooks (Oke 1987; Stull 1988; Bailey et al. 1997; Hupfer and Kuttler 2005). Therefore, the following chapter does not provide a comprehensive overview, but rather discusses some typical microclimatological phenomena. These phenomena are present under special weather situations, and influence the small-scale climate in typical ways. Many of these local effects are described only in regional publications. The impressive wind system of the foehn is not described because it exists on the larger meteorological scale.

7.1 Climatological Scales

The scales of climate are not as strict and uniform as those of meteorology, as proposed by Orlanski (1975). The term microclimate is often applied to space scales up to 100 m as in micrometeorology. It follows that mesoclimate has an extension of up to 100 km which is about one class of scales lower in comparison to Orlanski's (1975) classes in meteorology (Hupfer 1991). In the small-scale range, terms such as urban climate, topo or area climate (Knoch 1949), ecoclimate, local climate, and others are usual. A comparison of different classifications is given in Table 7.1, where the classifications by Kraus (1983), formerly used in the Western part of Germany, and Hupfer (1989) are most likely comparable to the classifications by Orlanski (1975). The term microscale is often used for the much smaller scales. In what was formerly East Germany, the microscale classification applied to scales below 1 m (Böer 1959).

Figure 7.1 is an illustration of the various climate scales and the phenomena associated with them. Microclimate is mainly associated with processes in the

T. Foken, *Micrometeorology*, DOI 10.1007/978-3-642-25440-6_7

Table 7.1 Classifications of climatological scales (Hupfer 1991)

km	Orlanski (1975)	Böer (1959)	Kraus (1983)	Hupfer (1989)
10^4	makro-β	Large climate	Macro range	Global climate
10^3	meso-α	range	Synopt. range	Zonal climate
10^2	meso-β		Meso-	Landscape climate
10^1	meso-γ	Local climate	range	
10^0	mikro-α	range	Micro range	Plot climate
10^{-1}	mikro-β		Topo range	Small scale climate
10^{-2}	mikro-γ			
10^{-3}		Micro climate		Border layer climate
10^{-4}		range		

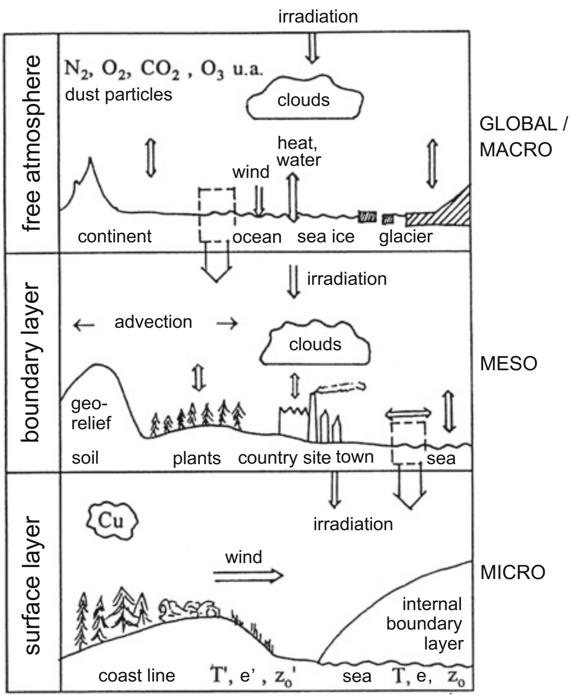

Fig. 7.1 The climate system in the macro, meso and micro scale (Hupfer 1996, adapted with kind permission of © Teubner Verlag Stuttgart, Leipzig 1996, All rights reserved)

surface layer, e.g. energy and matter exchange, radiation processes close to the ground surface, effects of the underlying surface, etc. However, cumulus convection is not considered a part of the microclimate.

7.2 Generation of Local Climates

7.2.1 Small-Scale Changes of Climate Elements

Microclimatological effects often result in strikingly different phenomena if the climate elements have pronounced differences for certain weather situations or at certain time periods. Elements such as global and diffuse radiation in the absence of clouds show little climatological differences; however, differences can occur in mountainous regions. Exceptions may occur if long-duration local circulation systems are connected with clouds (see Sect. 7.3). For example, in the summer cumulus clouds will develop only over the land during a land-sea breeze. In the winter, the opposite effect occurs, i.e. clouds develop over the warmer sea.

Large-scale pressure fields cause wind speed and direction; however, the topography or obstacles near the measurement site also influence the winds, and these can lead to small-scale climate differences. Similar effects occur for precipitation where differences often cannot be clearly separated from measurement errors.

Air temperature and moisture in a uniform air mass and at the same altitude show very little differences, except for nights with high longwave up-welling radiation and cooling. Thus, the temperature minima near the ground may show remarkable differences (see Sect. 7.4). Similar results are found for the net radiation, which may be very variable on small scales due to the dependence on the albedo and the surface humidity.

Relevant climate elements in microclimatology are listed in Table 7.2. It is shown under which circumstances hardly any microclimatologically-caused differences occur.

7.2.2 Local Climate Types

Local climate types can be generated due to small-scale circulations (see Sect. 7.3), due to wind shadows, a changed radiation regime and vegetation (Bailey et al. 1997; Bendix 2004; Foken 2013; Barry and Blanken 2016). The smallest influences on the local climate are found in agricultural landscapes. However, if the terrain is sloped the radiation budget is already non-uniform. Beneficial ***radiation climates*** are often found along the slopes of river valleys, which are used for viticulture. Drainage of cold air from elevated regions above the vineyard must be averted. Walls or trails are used to block or channel the cold air down the slope, and also to

Table 7.2 Microclimatological relevant climate elements

Climate element	Range and reason of microclimatological differences	Hardly microclimatological differences
Global and diffuse radiation	Hardly available	Unlimited horizon, free of typical local clouds
Net radiation	Partly significant due to differences in albedo and surface temperature	Unlimited horizon and uniform underlying surface
Wind velocity and wind direction	Partly significant in complex terrain and in the case of obstacles	Large fetch over uniform surfaces and no obstacles
Temperature (general) and air humidity	Often small	Open location
Minimum of the temperature, temperature near the surface, temperature of the upper soil layers	Partly significant, especially in valleys and hollows (also in very small scales)	Open location
Precipitation	Partly significant but mostly in the range of the measurement error	Open location

prevent pooling of cold air in the valley that could affect the vineyards. Therefore, the lowest part of the slope is often used for frost-resistant fruit trees.

A very interesting climate type is the ***forest climate***, as documented by the temperature observations in a forest shown in Fig. 3.3. The irradiation at day time heats up mainly the upper parts of the crown. Due to the stable stratification the cooler air from the night is still in the trunk space with a pleasant and often up to 5 degrees lower temperature. After sun set the top of the crown cools up by longwave up-welling radiation and the cooler air falls without a larger time lag into the trunk space. Nevertheless, the climate in the forest at night feels balmy in comparison to the surrounding of the forest, because the net longwave radiation in the trunk space is balanced. In the surrounding of the forest and on the top of the crown a larger cooling occurs.

The high heat capacity of water generates a special ***lake climate***, causing the surroundings of water bodies to be warmer during cold nights. This effect is most common in autumn. The ***climate of hollows*** is often quite uncomfortable. During the night, cold air can pool in the hollow. Due to wind sheltering the evaporation is typically low and the hollow feels cool and moist. In contrary, during days with intensive irradiation the air in a hollow can be excessively hot. Similar effects also occur in gullies, but there cold air outflow is often possible.

Even in gardens a special ***garden climate*** (Häckel 1989) may persist. For instance, hedges act as a windbreak and emit longwave radiation in the evening often causing balmy conditions in their surroundings. However, downwind of the windbreak, in its wake, the evaporation is reduced and these areas are moister with a tendency for growth of moss. Similar conditions prevail in rock gardens but in that case the high irradiation in the noon and afternoon hours is used to heat up the stones, which then act as a longwave heater at night. Windbreaks can increase this effect.

The ***urban climate*** has become a focus area (Kratzer 1956; Lietzke et al. 2015), also due to climate change research. Cold-air drainage (see Sect. 7.4) can have a strong effect on the urban climate. Because the buildings and streets within a city have high heat capacities, urban air cools more slowly at night than the surrounding rural areas leading to the formation of an *urban heat island*. If cold air is able to flow into a city, the heat island effect can be reduced. Green areas in cities are often very small and separated by buildings, and are therefore unable to produce enough cold air for the surrounding areas. Urban parks and grasslands should be larger than $200 \times 200\ m^2$ and humid (Spronken-Smith and Oke 1999; Spronken-Smith et al. 2000).

Therefore, the facility and the protection of park areas inside towns have a high relevance. Open forms, like the English garden type, should be preferred. Also with architectonical action and the application of special building material the heating can be reduced.

Of increasing relevance are measurements in street canyons (e.g., Klein and Clark 2007). An overview of such studies is presented in Appendix A.5. The objectives of these studies include investigating the energy and matter exchange in cities, also for air quality management, the influence of the buildings and open areas, and the carbon dioxide balance of towns (Kotthaus and Grimmond 2012).

The number of modelling (Best and Grimmond 2014) and experimental (see Appendix A.5) studies has significantly increased over the last years. Advanced, state-of-the-art modelling techniques (Letzel 2015) and measurement methods are widely applied to identify problems and to support the planning process.

Besides the importance of cold-air drainage in urban climates, the properties of the heat island are relevant. To investigate both, special measurements are necessary, as described in Sect. 7.6, because classical climate maps cannot describe all relevant processes. For special bioclimatological investigations, Table 7.3 gives some suggestions for assessment criteria by the superposition of heat, pressure, and ventilation (Gerth 1986).

Table 7.3 Superposition of criteria for a bioclimatological assessment (Gerth 1986)

	High	Moderate	Low
Bioclimatological pressure			
Heat pressure	>25 days	All other combinations	≤ 25 days
Wind velocity	$<2\ m\ s^{-1}$		$\geq 2\ m\ s^{-1}$
Frequency of inversions	$>30\%\ a^{-1}$		$\leq 30\%\ a^{-1}$
Ventilation			
Wind velocity	$\geq 2\ ms^{-1}$	All other combinations	$<2\ m\ s^{-1}$

7.3 Microclimate Relevant Circulations

7.3.1 Land-Sea Wind Circulation

Land-sea wind circulations arise form weak background winds and large temperature differences between land and sea. The heating over the land generates low-pressure areas with rising air. For compensation, cold air from the sea forms a sea breeze. Above the sea, resides a high-pressure area with descending air, i.e. subsidence. The sea breeze front penetrates inland distances ranging from a few decametres up to kilometres, and causes remarkable temperature differences over small areas, as illustrated in Fig. 7.2. After the beginning of the land-sea wind circulation, the temperature at the beach may be unpleasantly cool, while a little distance inland pleasant temperatures are found. During the night, these relations are opposite but less developed.

7.3.2 Mountain-Valley Circulation

Cooling during the night caused by radiation is the reason that cold air from mountaintops and slopes descends under gravity into valleys and fills cold-air reservoirs. If drainage winds pass through narrow valleys, a considerable katabatic wind can be occur. The strongest katabatic wind are found in Antarctica (King and Turner 1997). On smaller scales, katabatic flows have a significant role (see. Sect. 7.4).

During the day, the valley and the slopes are heated faster than the mountaintops (low wind velocities, less air exchange), and warm air moves upward along the slopes. These flows slowly lift the inversion layer until the mixed layer is fully developed. This process is illustrated in Fig. 7.3 following the classical paper by Defant (1949). The dispersion of the inversion is also possible by convective events from the centre of the valley (Brötz et al. 2014).

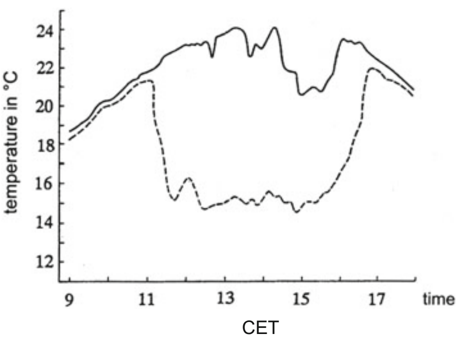

Fig. 7.2 Temperature cycle at the beach of Zingst (Baltic Sea, broken line) and 200 m inland with offshore wind of 4–7 ms^{-1} over land on May 17, 1966 according to Nitzschke (1970, adapted with kind permission of © WILEY-VCH Verlag Weinheim 1970, All rights reserved)

Fig. 7.3 Schematic view of the mountain-valley circulation (Adapted from Stull 1988, with kind permission of © Kluwer Academic Publisher B. V. Dordrecht 1988, All rights reserved)

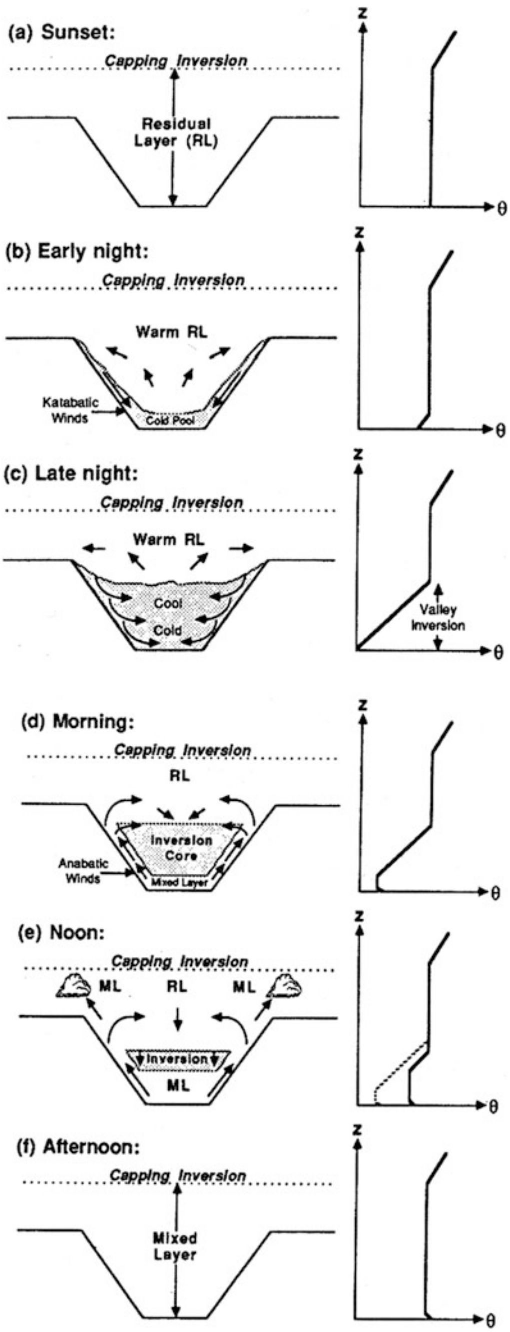

The strength of the katabatic wind can be determined from the temperature difference between the cold air flowing downslope and the surrounding area. Applying a local equilibrium between buoyancy and stress the velocity of the katabatic flow is (Stull 2000)

$$u_k = \left(\frac{g \cdot (T - T_k)}{T} \cdot \frac{h}{C_D} \cdot \sin \alpha \right)^{1/2} \tag{7.1}$$

h is the depth of the cold air layer, C_D is the drag coefficient, α is the angle of inclination of the slope, g is the acceleration due to gravity, T is the surrounding air temperature, and T_K is the temperature of the cold air layer. Also, Eq. (7.1) can be added as a buoyancy term into the Navier-Stokes equation Eq. (2.1).

7.4 Local Cold-Air Flows

Cold-air flows are the most common microclimatological phenomenon (VDI 2003). Source areas include, for example, open hilltops, forested slopes, and other inclined surface areas. The cold-air flow can be imagined as a flow of compact air parcels that can be interrupted or damped by obstacles. With a trained eye, the relevant cold-air flows can be localized according to the form of the landscape and the vegetation. This assessment can be made using a classification. Steps of the classification are detailed in Tables 7.4 and 7.5. The verifications can be made with well-aimed measurements (see Sect. 7.6). At very high risk, are cold air nights with strong longwave radiation due to cloudless skies. This is especially the case following synoptically-caused cold air advection (e.g. Three Saints' Days, a European weather phenomenon occurring in May). Two useful preventive measures are sprinkling with water so that more energy is necessary for the freezing of the water droplets, and fogging with smoke so that the cooling by long-wave radiation is above the plant canopy.

An impressive example of a small-scale cold-air flow is shown in Fig. 7.4. At the morning of May 04, 2011 a very significant late frost event occurred in Germany under clear sky after the inflow of fresh cold air. At a meadow slope with 200 m length and 40 m height difference temperatures measured at 5 cm above the surface at the bottom of the valley and the top of the slope differed by 6 K. At a

Table 7.4 Classification of the frost risk (cloudiness < 2/8, wind velocity < 3 ms^{-1}) according to Schumann (personal communication)

Risk class	Indication	Comparison to normal conditions
1	Favored	+1 to +5 K
2	Normal condition	−1 to +1 K
3	Weak to moderate frost risk	−2 to −4 K
4	High to very high frost risk	−5 to −8 K

Table 7.5 Risk class according to the profile of the terrain according to Schumann (personal communication)

Relief form	Cold air inflow, production	Cold air drainage	Risk class[a]
Closed basin	Existing	–	3
Ground of the valley, low slope	Existing	Weak	3
Ground of the valley, moderate slope	Existing	Moderate	3
Plates, Δh > 10 m	–	–	2
Slope, low inclination (1–3°)	–	Moderate	2
Slope, high inclination (>15°)	–	Very good	1
Hills h > 50 m, inclination > 10°	–	Very good	1

[a]marshy soil +1

nearby hill that was only 175 m above the bottom of the valley ground frost was weak and the temperature at 2 m height was above 0 °C, while in the valley the temperature was – 5 °C. Interestingly, the temperature in the valley increased at 03:30 local time, while the next higher measurement point had the lowest temperature, which can be explained by the formation of ground fog. Fog formation and breakup also caused temperature variations in the following hours. Such local cold air hazards can be easily detected by visual inspection.

Cold-air generation in valleys augmented by cold-air drainage can lead to radiation fog if the air is cooled below its dew point. After the generation of the fog, the strongest cooling by radiation occurs at the top of the fog. Because of this, the coldest temperatures are no longer found in the valley but along the slopes above the fog, as shown in the example above. The reduced longwave radiation from the ground causes a lifting of the fog, and in the low radiation season this is the reason for daylong low stratus within closed valleys or basins.

A special form of the fog is sea smoke, a cumulus-like cloud of some meters in thickness. This is generated by cold air flowing over warmer water. Because this convective effect can happen only for water-air temperature differences greater than 10 K (Tiesel and Foken 1987), sea fog occurs by advection of cold air most often in late spring, when small lakes are already warm, or in autumn and early winter over large lakes or the oceans.

7.5 Land Use Changes and Local Climate

Land use changes play nowadays an important role, because they significantly influence the local climate but may also affect the whole climate system in the case of changes over large areas (Cotton and Pielke Sr 2008; Mölders 2012). In this chapter examples of typical changes are shown. However, estimating the effect of

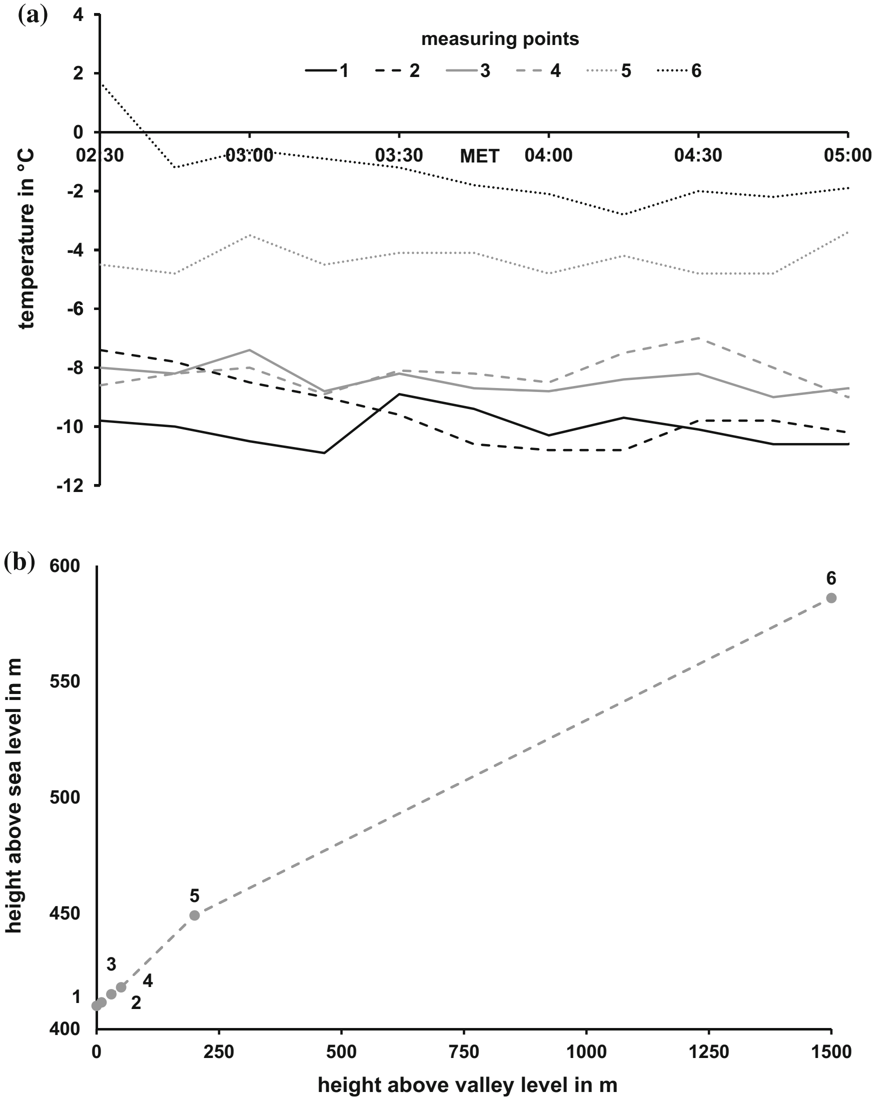

Fig. 7.4 Temperature **a** measured at 5 cm above the surface in the morning of May 04, 2011 near Frankenhaag (region Bayreuth, Germany) at 5 measurement points distributed along a slope as illustrated in the schematic height profile **b.** The sites were at the bottom of the valley (*1*), above a meadow (*2*–*4*), at a forest edge (*5*), and on the top of a nearby hill (*6*). Sun rise was at 04:45 MET. The data were collected during experiments with students of the University of Bayreuth

typical land use changes is not always simple, because the relationships are largely non-linear. Estimating the effects of roughness changes is most simple, while for albedo changes the relationships are extremely complex. Figure 7.5 illustrates the complexity of this question.

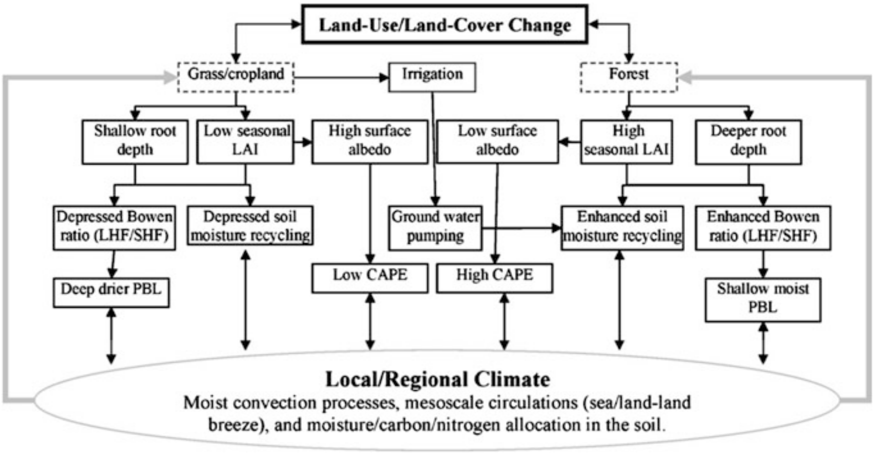

Fig. 7.5 Schematic illustration of the influence of land use and land cover changes on the local and regional climate (Adapted from Pielke Sr et al. 2007, with kind permission of © Elsevier AG Oxford 2004, All rights reserved)

7.5.1 Changes of Surface Roughness

Changes of the surface roughness are very common, e.g. due to deforestation, housing development, soil sealing. The implications can be easily estimated with Eq. (2.87), i.e. a reduction of the roughness length is related to an increase of the wind velocity. Given the proportionality of wind and friction velocity and of the roughness heights for momentum and scalars it also follows according to Eq. (2.90) that the fluxes of scalars increase. Because evaporation needs a lot of energy, which can be provided e.g. by a downward sensible heat flux (oasis effect), and the wind velocity may be high in the case of neutral stratification, an increase of the evaporation is possible. High wind velocities and a dehydration of the soil are the basis for erosion. This is very relevant in areas with fine-grained soil, like sand or loess. In areas with high wind velocities, like Great Britain or Northern Germany, the erosion potential was reduced by windbreaks (hedges or stone walls) already in ancient times. It is interesting that the typical distances are of the order of 100 m, which agrees well with the wind reduction zone due to internal boundary layer development (see Sect 3.2).

On the other hand, reduction of the wind velocity also occurs due to urban sprawl. However, the sensible heat flux often does not drastically decline, because the lower wind velocities and the shortwave down-welling radiation promote stronger heating of the surface and subsequently also an increase in air temperatures. Because the largest roughness elements dominate the roughness of an area, large wind farms reduce the wind velocity. This is of particular relevance for off-shore wind farms, where the effect is very large due to the low roughness of the ocean (Witha et al. 2014). Consequently, wind turbines are installed on the ocean and on mountain hills like pearl necklaces, perpendicular to the mean wind direction. Above forests, the applicability of the relationship between wind velocity and roughness is limited due to the generation of an mixing layer (see Sect 3.5.3).

7.5.2 Changes of the Evaporation

In some parts of the World, actions to reduce the evaporation are already in use. A successful strategy has been to increase the surface roughness by using wind breaks, such as hedges and stonewalls, or groups of trees, such as savannahs and orchards, in more open landscapes which, in these cases, suppresses the evaporation from the soil or grass. Such measures will gain in importance due to climate change.

Very critical are the reduction of the evapotranspiration due to deforestation mainly in tropical regions but also due to the wide-spread urban sprawl and related sealing of large areas. The related environmental impacts on the water balance of the Earth are significant and the proportion of arid areas continues to rise. The preservation of natural forests with high carbon uptake and resistance to extreme weather events has a special significance (Herbst et al. 2015).

But also the extraction of water in arid areas is important. Thereby dew is a source for plants and animals which should not be underestimated. Open areas provide favourable conditions for dew formation as air quickly cools down in the case of low wind velocities and longwave up-welling radiation. This is e.g. the case in open savannah areas where dew formation in the morning is an important source of water for ground vegetation and animals. The increasing areas of scrublands counteract this effect. In a closed scrubland the top of the scrubs cools and the cold air sinks down, but the dew point temperature will not be reached at the surface. Therefore, fire-clearing is often applied.

7.5.3 Change of the Albedo

Changes of the albedo are discussed controversially. Often it is assumed that an increase of the albedo increases the reflected shortwave radiation which reduces the shortwave radiation balance (Davin and de Noblet-Ducoudré 2010). It is then argued that the energy loss caused by the higher reflection of shortwave radiation results in decreasing sensible heat fluxes and thus a cooling effect.

By comparison of Tables 1.2 and 1.4 with albedo and soil heat capacity data, respectively, it is obvious that an increase in albedo comes along with a brighter and dryer surface and thus also a lower heat capacity. It is true that the reflected shortwave radiation increases, but due to the lower heat capacity of the soil less energy is stored. Furthermore, since heat conductance also is low the ground heat flux is reduced. Therefore, a very thin top layer of the soil strongly heats up causing the sensible heat fluxes and longwave upwelling radiation to rise. Furthermore, the erosion potential increases. The problem is very complex and expert studies often must rely on models, in which land-surface processes and atmospheric interactions are well parameterized.

Changes of the albedo have the most prominent effects in Arctic and Antarctic regions. Due to the melting of the sea ice the change can be, in the extreme case, from 95 to 5% and substantial amounts of energy can be stored in the water of the ocean. This increases the evaporation, which is much higher than the sublimation from the ice, with implications on cloudiness and precipitation patterns. Additionally, the deposition of dust and soot due to the increasing commercial utilisation of these areas and the thawing of ice surfaces are reasons for significant changes of the albedo. Also, on land areas the snowmelt suddenly changes the energy distribution (Westermann et al. 2009). Changes of the albedo in polar regions and the deforestation of the tropical rain forests have the strongest influence on the earth's climate.

7.5.4 Degradation

The degradation of the vegetation cover of soils if of great concern, particularly in sensitive and slowly growing ecosystems like alpine meadows, but also in areas with agricultural depletion or areas which will be drier due to climate change. Reasons are overgrazing, erosion, landslides, dehydration, degradation due to small rodents and similar factors. The effects can be of complex nature including a release of carbon dioxide from the exposed soil, the increase of the sensible heat flux over bare soils with a change of the Bowen ratio and the albedo. By the change from the plant covered to the non-plant covered surface there is a change from evapotranspiration to evaporation. Due to the missing regulation of the plants the water evaporates earlier on the day with earlier cloud generation and precipitation (Babel et al. 2014). Analogue to albedo changes, only careful modeling studies and validation experiments can provide insight about the complex and non-linear mechanisms.

7.6 Microclimatological Measurements

Microclimatological measurements have a high relevance for consulting activities (see Sect. 8.2.5). They are necessary for urban and health-spa climate assessments. Also, many applications are found in agriculture, for example assessing frost risk in orchards and vineyards. Engineers with different degrees of experience often make these assessments. Assessments made using single situations are not sufficient for a generalization. It is important to find those processes that are relevant to the observations. Therefore, the special conditions of the near-surface layer discussed in Chap. 3 must be taken into account. Predominantly, only relevant state parameters are mapped out, e.g. cold-air flows or the heating of city centres. Typically, simple measurements (temperature, see Sect. 7.4; smoke experiments) are used which do not provide data for important parameters such as the volume flow. There are only a few approaches where atmospheric stability and turbulent fluxes are considered. These are important parameters that must be compared for instance in assessing deposition potential.

Microclimatological measurements cannot be done independently from climatologically measurements. This means that climatologically measurements must be made first. This requires the selection of a relevant basic climate station with measurements over many years and made by meteorological services. Furthermore, measurements in the area of investigation over 1–2 years are necessary to transfer the climatological data to this area. Such station can be a small automatic weather station, which should be placed at relevant points according to the classification of the landscape. The real microclimatological measurements are made with moving instrument packages such as cars, vans etc. or intensive field campaigns. Therefore, it is necessary that a weather situation must be chosen during which the phenomena being investigated are clearly seen. For cold-air risk investigations, clear nights after cold air advection are necessary. During these mobile measurements, the vehicles stop at the relevant measurement stations to correct the temporal trends. Mobile measurements can be supported by thermal pictures from aircraft. These are not alternatives to mobile measurements because of the missing wind information, which is important for the dynamics of the processes. Otherwise, there is a risk that single measurements can be over interpreted, which are absolutely different for other wind conditions. For visualizations, lasers and recently also fibre optic systems can be applied, while the latter method offers a direct temperature measurement (Zeeman et al. 2015).

Vertical soundings of the atmospheric boundary layer with balloons or indirect measurement techniques (sodar, lidar, passive remote sensing techniques in the infrared or microwave spectrum) may be useful. The aim is to study the local development of inversion layers and therefore the dilution of emitted air pollutions and depth of the exchange volume.

In heavily built up areas, radiation measurements are also necessary, e.g. the measurements of the reflected shortwave radiation or the longwave emitted radiation close to buildings. Because of climate change, these effects have an increasing relevance during hot summer days. In the last few years, the contribution of turbulent fluxes has not only been better understood, but also measured in many urban experiments. Appendix A.5 gives an overview about such experiments in the last years. Special problems are the determination of the zero-plane displacement height (see Sect. 3.1.2) and of the exact footprint (see Sect. 3.4.3, Leclerc and Foken 2014).

References

Babel W, Biermann T, Coners H, Falge E, Seeber E, Ingrisch J, Schleuß PM, Gerken T, Leonbacher J, Leipold T, Willinghöfer S, Schützenmeister K, Shibistova O, Becker L, Hafner S, Spielvogel S, Li X, Xu X, Sun Y, Zhang L, Yang Y, Ma Y, Wesche K, Graf HF, Leuschner C, Guggenberger G, Kuzyakov Y, Miehe G and Foken T (2014) Pasture degradation modifies the water and carbon cycles of the Tibetan highlands. Biogeosci. 11:6633-6656.

Bailey WG, Oke TR and Rouse WR (eds) (1997) The Surface Climate of Canada. Mc Gill-Queen's University Press, Montreal, Kingston, 369 pp.

Barry R and Blanken P (2016) Microclimate and Local Climate. Cambridge University Press, Cambridge, 316 pp.

Bendix J (2004) Geländeklimatologie. Borntraeger, Berlin, Stuttgart, 282 pp.

Best MJ and Grimmond CSB (2014) Key conclusions of the first international urban land surface model comparison project. Bull Amer Meteorol Soc. 96:805–819.

Böer W (1959) Zum Begriff des Lokalklimas. Z Meteorol. 13:5–11.

Brötz B, Eigenmann R, Dörnbrack A, Foken T and Wirth V (2014) Early-morning flow transition in a valley in low-mountain terrain. Boundary-Layer Meteorol. 152:45–63.

Cotton WR and Pielke Sr RA (2008) Human Impacts on Weather and Climate. Cambridge University Press, Cambridge, 320 pp.

Davin EL and de Noblet-Ducoudré N (2010) Climatic impact of global-scale deforestation: Radiative versus nonradiative processes. J Climate. 23:97–112.

Defant F (1949) Zur Theorie der Hangwinde, nebst Bemerkungen zur Theorie der Berg- und Talwinde. Archiv Meteorol Geophys Bioklim, Ser. A. 1:421–450.

Foken T (2013) Energieaustausch an der Erdoberfläche. Edition am Gutenbergplatz, Leipzig, 99 pp.

Gerth W-P (1986) Klimatische Wechselwirkungen in der Raumplanung bei Nutzungsänderungen. Ber Dt Wetterdienstes. 171:69 pp.

Häckel H (1989) Das Gartenklima. Ulmer, Stuttgart, 128 pp.

Herbst M, Mund M, Tamrakar R and Knohl A (2015) Differences in carbon uptake and water use between a managed and an unmanaged beech forest in central Germany. For Ecol Managem. 355:101–108.

Hupfer P (1989) Klima im mesoräumigen Bereich. Abh Meteorol Dienstes DDR. 141:181–192.

Hupfer P (ed) (1991) Das Klimasystem der Erde. Akademie-Verlag, Berlin, 464 pp.

Hupfer P (1996) Unsere Umwelt: Das Klima. B. G. Teubner, Stuttgart, Leipzig, 335 pp.

Hupfer P and Kuttler W (eds) (2005) Witterung und Klima, begründet von Ernst Heyer. B. G. Teubner, Stuttgart, Leipzig, 554 pp.

King JC and Turner J (1997) Antarctic Meteorology and Climatology. Cambridge University Press, Cambridge, 409 pp.

Klein P and Clark JV (2007) Flow variability in a North American downtown street canyon. J Appl Meteorol Climatol. 46:851–877.

Knoch K (1949) Die Geländeklimatologie, ein wichtiger Zweig der angewandten Klimatologie. Ber Dtsch Landesk. 7:115–123.

Kotthaus S and Grimmond CSB (2012) Identification of micro-scale anthropogenic CO_2, heat and moisture sources—Processing eddy covariance fluxes for a dense urban environment. Atmos Environm. 57:301–316.

Kratzer (1956) Das Stadtklima. Vieweg, Braunschweig, 184 pp.

Kraus H (1983) Meso- und mikro-skalige Klimasysteme. Ann Meteorol. 20:4–7.

Leclerc MY and Foken T (2014) Footprints in Micrometeorology and Ecology. Springer, Heidelberg, New York, Dordrecht, London, XIX, 239 pp.

Letzel MO (2015) Urban large-eddy simulation (LES), Advanced computational fluid dynamics for urban climatic maps. In: Ng E and Ren C (eds.), The Urban Climatic Map: A Methodology for Sustainable Urban Planning. Routledge, 421–428.

Lietzke B, Vogt R, Young DT and Grimmond CSB (2015) Physical fluxes in urban environment. In: Chrysoulakis Net al (eds.), Understanding Urban Metabolism. Routledge, Abingdon, New York, 29–44.
Mölders N (2012) Land-Use and Land-Cover Changes, Impact on climate and air quality. Springer, Dordrecht, Heidelberg, London, New York, 189 pp.
Nitzschke A (1970) Zum Verhalten der Lufttemperatur in der Kontaktzone zwischen Land und Meer bei Zingst. Veröff Geophys Inst Univ Leipzig. XIX:339–445.
Oke TR (1987) Boundary Layer Climates. Methuen, New York, 435 pp.
Orlanski I (1975) A rational subdivision of scales for atmospheric processes. Bull. Am. Meteorol. Soc. 56:527–530.
Pielke Sr RA, Adegoke JO, Chase TN, Marshall CH, Matsui T and Niyogi D (2007) A new paradigm for assessing the role of agriculture in the climate system and in climate change. Agrical Forest Meteorol. 142:234–254.
Spronken-Smith RA and Oke TR (1999) Scale modelling of nocturnal cooling in urban parks. Boundary-Layer Meteorol. 93:287–312.
Spronken-Smith RA, Oke TR and Lowry WP (2000) Advection and the surface energy balance across an irrigated urban park. Int J Climatol. 20:1033–1047.
Stull RB (1988) An Introduction to Boundary Layer Meteorology. Kluwer Acad. Publ., Dordrecht, Boston, London, 666 pp.
Stull RB (2000) Meteorology for Scientists and Engineers. Brooks/ Cole, Pacific Grove, 502 pp.
Tiesel R and Foken T (1987) Zur Entstehung des Seerauchs an der Ostseeküste vor Warnemünde. Z Meteorol. 37:173–176.
VDI (2003) Umweltmeteorologie, Lokale Kaltluft, VDI 3787, Blatt 5. Beuth-Verlag, Berlin, 86 pp.
Westermann S, Lüers J, Langer M, Piel K and Boike J (2009) The annual surface energy budget of a high-arctic permafrost site on Svalbard, Norway. The Cryosph. 3:245–263.
Witha B, Steinfeld G, Dörenkämper M and Heinemann D (2014) Large-eddy simulation of multiple wakes in offshore wind farms. J Phys: Conf Ser. 555: 012108.
Zeeman M, Selker J and Thomas C (2015) Near-surface motion in the nocturnal, stable boundary layer observed with fibre-optic distributed temperature sensing. Boundary-Layer Meteorol. 154:189–205.